

WHITE DWARF EVOLUTION AND CRYSTALLIZATION

O.G. BENVENUTO* and L.G. ALTHAUS**

Facultad de Ciencias Astronómicas y Geofísicas, Universidad Nacional de La Plata, Paseo del Bosque S/N (1900) La Plata, Argentina. Email: obvenuto@fcaglp.fcaglp.unlp.edu.ar

(Received 24 October, 1994; accepted 4 July, 1995)

Abstract. We present a numerical study for the evolution of non-DA white dwarfs of 0.4, 0.55, 0.8, 1.0, and $1.2M_{\odot}$. We pay special attention to the behaviour of the crystallization front. It is shown that crystallization begins at higher luminosities the higher the white dwarf mass is. The shape of the crystal growth function is very similar, almost independent of the value of the total stellar mass. We also study the crystallization process analytically, finding that it is nicely reproduced by a very simple model that accounts for the numerical results.

1. Introduction

It has been known for some time (Mestel and Ruderman, 1967; Van Horn, 1968; Lamb and Van Horn, 1975) that Coulomb interactions make white dwarf (WD) stars begin to develop a crystalline core at a certain luminosity L_o which depends upon the WD mass and its chemical composition. From that moment on, the crystallization front moves outwards reaching the outer layers in a relatively narrow range of luminosities. Crystallization affects WD evolution in two ways. First, this process causes the release of latent heat retarding the evolution. Second, the specific heat of matter is modified.

After crystallization, the star enters the Debye phase. During this phase, the WD becomes cool in a short time scale due to a fast depletion of the thermal content as the central temperature decreases (D'Antona and Mazzitelli, 1989). For recent reviews on the physics and cooling of WDs see Koester and Chanmugam (1990) and D'Antona and Mazzitelli (1990) respectively; see also Shapiro and Teukolsky (1983).

It is the purpose of this work to describe this important stage in WD life by means of a detailed numerical simulation of the process. Also, we present a simple analytic treatment for calculating the growth of the crystal phase. Our WD evolutionary code is presented in Section 2, where we describe the main physical ingredients we have taken into account. In Section 3, we show the results of our simulations for the WDs we have considered. In Section 4, we present the analytic treatment for the growth of the crystal phase and Section 5 is devoted to the discussion and conclusions.

* Member of the Carrera del Investigador Científico, Comisión de Investigaciones Científicas de la Provincia de Buenos Aires (Argentina).

** Fellow of the Consejo Nacional de Investigaciones Científicas y Técnicas (Argentina).

2. The Evolutionary Code

In this section, we summarize the main characteristics of our evolutionary code. It has been written independently of other researchers (Benvenuto, 1988) following the method of Kippenhahn, Weigert, and Hofmeister (1967). Neutrino emission processes (Itoh and Kohyama, 1983a; Itoh *et al.*, 1989, 1992; Munakata *et al.*, 1987) as well as latent heat released during crystallization are considered. A detailed equation of state has been carefully taken into account: briefly, at high densities, where matter is completely ionized, ideal gas, Coulomb interactions, and quantum liquid contributions have been taken from Hansen (1973); electron exchange and Thomas-Fermi corrections for finite temperature were also included following the procedure given by Shaviv and Kovetz (1972) and Kovetz *et al.* (1972). The specific heat for the ions in the solid phase have been computed following the recent treatment given by Chabrier (1993). At low densities we employed the equation of state developed by Magni and Mazzitelli (1979) where a partially ionized, partially degenerate plasma subject to Coulomb interactions is considered.

Convection has been included following the Mixing Length theory. The ratio of mixing length to pressure scale height has been chosen to be $l/H_p = 1.5$.

Concerning conductive opacities, we included the analytic fitting formulae given in Iben (1975) for the low density regime. Those fits are based on the calculations of Hubbard and Lampe (1969). For the high density regime, we followed the works of Itoh and collaborators (1983b, 1984, 1993). Radiative opacities κ_r were taken from Cox and Tabor (1976) for the low metal abundance ($Z = 10^{-5}$) case. When values of κ_r are needed outside the tabulated region, linear extrapolations of $\log \kappa_r$ at constant temperature are employed. We have not taken into account the newer opacity data given in Rogers and Iglesias (1992), Iglesias *et al.* (1992), and Iglesias and Rogers (1993) because in the conditions attained in the WD envelope, we would need to extrapolate farther compared to Cox and Tabor's (1976) data.

Crystallization has been assumed to occur when the plasma coupling constant Γ reaches the value $\Gamma_m = 160$, where

$$\begin{aligned} \Gamma &\equiv \frac{Z^2 e^2}{kT \langle r \rangle} \\ &= 2.2697 \times 10^5 \frac{\rho^{1/3}}{T} \sum_i X_i Z_i^2 A_i^{-1/3} \end{aligned} \quad (1)$$

where $\langle r \rangle$ is the mean interparticle distance, and X_i being the abundance by mass of an ion of atomic mass A_i and charge Z_i . However, more recent studies seem to indicate a larger value for the onset of crystallization (for instance, Ogata and Ichimaru, 1987 obtained $\Gamma_m = 180$). Due to this uncertainty, Γ_m is regarded as a free parameter (Koester and Chanmugam, 1990), and the value 160 has been used up to now in almost all relevant cooling calculations (see, for example, D'Antona and Mazzitelli, 1989). It is worth mentioning, that in our computations we have

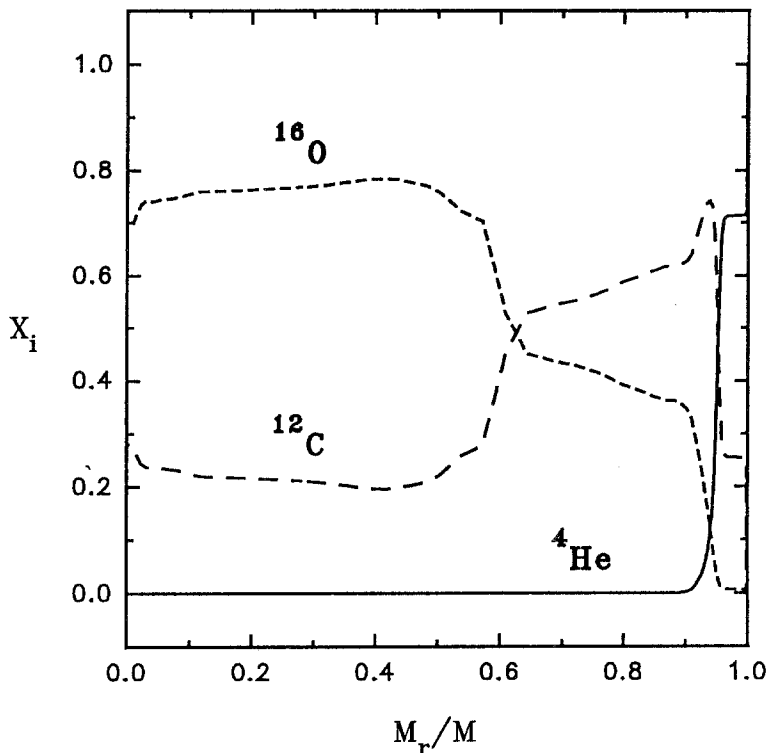


Fig. 1. The chemical composition of models vs. the fractional mass. Solid line corresponds to ${}^4\text{He}$, medium dashed lines to ${}^{12}\text{C}$ and short dashed lines to ${}^{16}\text{O}$.

not performed any free – energy minimization to calculate the thermodynamic conditions at the solid – liquid phase transition.

3. Numerical Results

We have evolved five WD models with masses of $M/M_{\odot} = 0.4, 0.55, 0.8, 1,$ and 1.2 all of them with the same chemical stratification shown in Figure 1. This is a Carbon-Oxygen core surrounded by an almost pure helium layer. This chemical profile has been calculated by D’Antona and Mazzitelli (1989) for the pre-WD evolution of a $0.55M_{\odot}$ WD model. We have assumed the same chemical composition for all our models (except for the models included in Figure 7), in spite of the fact that changes should be expected because of the differences in the evolution of progenitor objects. We would need, in order to improve our assumption, calculations of the pre-WD evolution of these objects. At present such calculations are not available.

We have chosen a non-DA chemical profile in order to avoid mixing episodes during crystallization that indeed occur if we allow for an external hydrogen layer

(Benvenuto and Althaus, in preparation). This would induce discontinuities in the $\log T_c - \log L/L_\odot$ relationship that would complicate the analysis we want to perform.

The models were evolved from $\log L/L_\odot = 0$ to $\log L/L_\odot \approx -5.5$ in sequences of about 1000 timesteps and divided in approximately 2000 mesh-points. Because the luminosity of the starting model we received from D’Antona and Mazzitelli is somewhat low ($\log L/L_\odot \approx -1.7$), we performed a kind of “artificial evolution” (see Kippenhahn *et al.*, 1967 for some other useful techniques) in order to begin our evolutionary calculations at higher luminosities. In broad outline, we have incorporated an artificial, constant specific energy generation for the entire model, which has been increased progressively until the WD reaches a luminosity (approximately $\log L/L_\odot = 1$) far larger than the initial model considered here. Then we turned it off smoothly, fast enough to reach $L = L_\odot$ with no contribution of this artificial procedure. The transitory state of the WD interior is damped out, and we get a plausible initial structure for our WDs. We want to mention that we have examined the thermal structure of the $0.55M_\odot$ model before and after the quoted procedure finding that the variations of pressure and temperature ($\delta P/P$ and $\delta T/T$), in a shell by shell comparison, were less than 1%; only in a narrow range of the mass coordinate located in the outer envelope, $\delta T/T$ reached $\approx 5\%$ which shall evidently not affect the results of this work.

In order to construct the 0.4 , 0.8 , 1.0 , and $1.2M_\odot$ initial models from the D’Antona and Mazzitelli one, we employed the same kind of method as described above but now the total mass of the model is changed (at constant fraction, i.e. $\delta M/M = \text{const}$) little by little during the artificial “heating” up to reach the definitive mass of the model before the maximum luminosity is reached. Then, after the beginning of the cooling, the transient effects are damped out before the model reaches the maximum luminosity considered as meaningful in the present work.

First, let us show the regions in the Hertzsprung-Russell diagram where crystallization and neutrino emission represent the most important episodes in WD life as well as the cooling tracks of the models. They are depicted in Figure 2 together with the lowest part of the Zero Age Main Sequence calculated by D’Antona and Mazzitelli (1994) for stars from 0.08 to $1M_\odot$, shown for the sake of comparison. Our WD stars evolve at almost constant radii as expected for a configuration subject to strong degeneracy. Note that due to the famous mass-radius relation (Chandrasekhar, 1939), at a given effective temperature the greater the mass, the lower the luminosity.

From this Figure, it is evident that neutrino emission is the dominant cooling mechanism during the initial hot phases of WD evolution. However, neutrino emission becomes negligible below $\log L/L_\odot \approx -1.5$. Specifically, we have denoted the neutrino luminosity L_ν of the models when $L_\nu = 10^{-1}$, 10^{-2} , and $10^{-3}L_\odot$. It is clear that massive WDs fade away in neutrinos at much higher photon

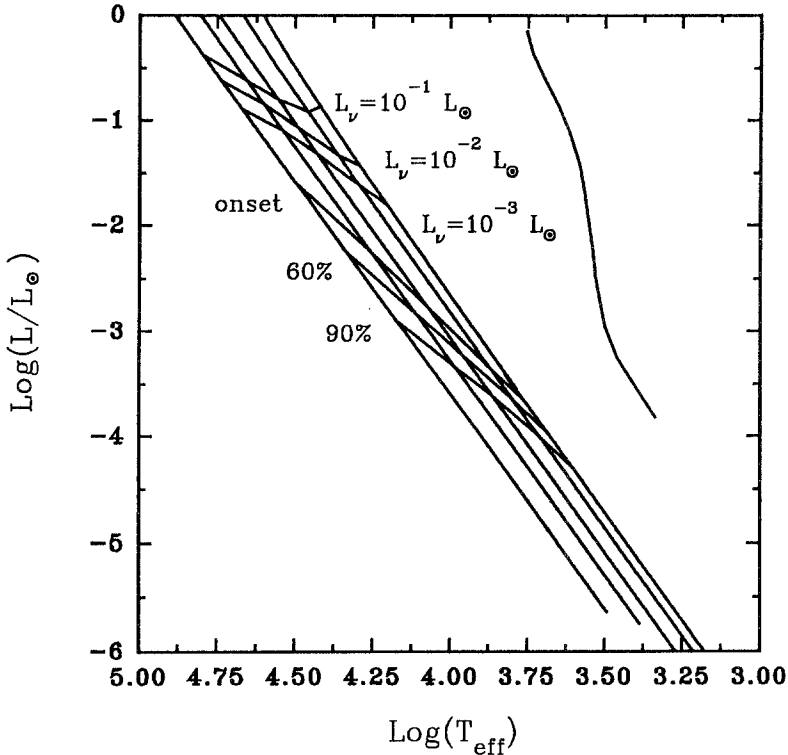


Fig. 2. The Hertzsprung-Russell diagram. From right to left, tracks corresponding to models with $M = 0.4, 0.55, 0.8, 1,$ and $1.2M_{\odot}$ are depicted. We also show the location of the onset of crystallization, and the moment when it embraces 60% and 90% of the stellar mass. The locus for the neutrino luminosities $L_{\nu} = 10^{-1}, 10^{-2}$ and $10^{-3}L_{\odot}$ are also denoted. For the sake of comparison we include the ZAMS for low mass stars given in D'Antona and Mazzitelli (1994).

luminosities than low mass ones. Also, the onset of crystallization, and the moment when the crystal phase embraces 60 and 90% of the stellar mass are indicated.

In Figure 3 we show the fraction of crystallized mass vs. luminosity relation for each model. As the models evolve, their interiors become cooler and at a given luminosity, which depends upon the stellar mass and chemical composition, a crystalline core appears and begins to grow ($\Gamma \geq 160$). It is evident that for large masses, crystallization sets in earlier due to their larger central densities. For instance, the model with $1.2M_{\odot}$ begins to crystallize when its luminosity is about 100 times as high as the luminosity of crystallization onset for the $0.55M_{\odot}$ model. This fact makes the effect of the released latent heat on cooling times be relatively more important for low mass objects. A similar result is also obtained by Wood (1992).

It can be realized from Figure 3 that the growth of the crystal phase is rather similar for all WDs here considered, despite the fact that they differ in masses up to a factor of three. This function is very smooth from $M_{\text{cryst}}/M = 0$ to

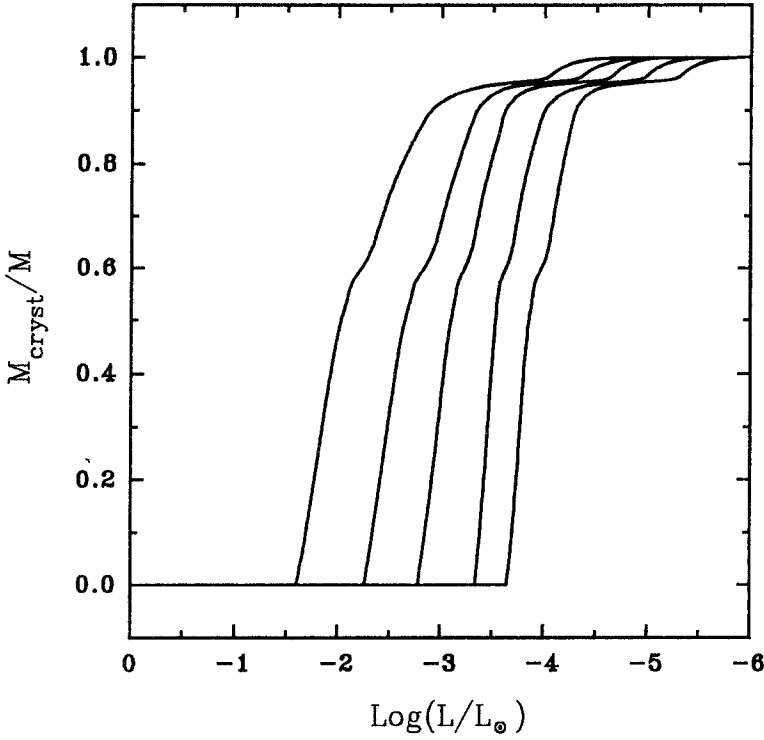


Fig. 3. The evolution of the crystallization front in the Lagrangian coordinate as a function of the luminosity. It can be noticed that the growth of the crystallized core follows a similar trend, though it begins at higher luminosities the higher the stellar mass is.

≈ 0.6 where the chemical composition profile changes abruptly. From there on, it again proceeds smoothly up to $M_{\text{cryst}}/M \geq 0.9$ where the helium rich outer layer envelope is reached.

As shown by Liebert, Dahn, and Monet (1988) the observed luminosity function for WD stars exhibits an abrupt falloff at $\log L/L_{\odot} \approx -4.5$. Our results predict that the objects located at this falloff should be almost completely solid as shown long ago by several authors (see e.g. Van Horn, 1968; Lamb and Van Horn, 1975).

Although the present paper is intended mainly to describe the behaviour of crystallization front, we give in Table II some additional results from our evolutionary calculations corresponding to the model with $0.55M_{\odot}$ (and pure helium envelope). This value for the mass is very close to the peak of the mass distribution obtained by Bergeron *et al.* (1992) (we are currently carrying out a more detailed study of these results which will be presented in a following publication). In Table II are listed, from left to right, photon luminosity, neutrino luminosity, effective temperature, central temperature, central density, fraction of crystallized mass, thickness in mass fraction of the convective envelope, and age.

TABLE I
Values of α for different masses

M/M_{\odot}	α
0.40	1.60
0.55	1.50
0.80	1.90
1.00	2.28
1.20	2.37

4. The Analytical Model

In this section, we present a simple Mestel-like (Mestel and Ruderman, 1967; Van Horn, 1968; Shapiro and Teukolsky, 1983, Chapter 4) analytical method to describe the behaviour of the crystallization front as a function of luminosity. We begin with the assumption that the opacities in the non-degenerate, radiative envelope can be characterized by a Kramers law opacity

$$\kappa = \kappa_o \rho T^{-\alpha}, \quad (2)$$

and that this envelope surrounds a degenerate, isothermal interior at temperature T_* . It can easily be shown (see e.g. Shapiro and Teukolsky, 1983, Chapter 4 for the case of Kramers opacity) that the luminosity is given by

$$L = \frac{2.11 \times 10^{31}}{5 + \alpha} \frac{\mu}{\mu_e^2} \frac{1}{\kappa_o} \frac{M}{M_{\odot}} T_*^{\alpha}, \quad (3)$$

where μ and μ_e are the mean molecular weight per particle and per electron respectively. If we assume Kramers opacities, we have $\kappa_o = 4.34 \times 10^{24} Z(1 + X)$ and $\alpha = 3.5$ (Schwarzschild, 1958) where X and Z are the mass fraction of hydrogen and heavy elements in the non-degenerate envelope respectively.

From Equation (1) we can estimate the *melting temperature* ($\Gamma = 160$) as

$$T_{\text{cryst}} = 1.418 \times 10^3 Z^2 A^{-1/3} \rho^{1/3}, \quad (4)$$

for a given composition, that we shall assume to be the same throughout the WD interior.

Let us employ a simple gaussian approximation for the density profile of the WD interior

$$\rho = \rho_0 \exp -(r/a)^2, \quad (5)$$

where ρ_0 is the central density and a the typical size of the WD, both depending upon the WD mass. As it can be noticed from Figure 4, this is a very good

TABLE II
Selected stages of the evolution of a 0.55 WD

$\log(L/L_{\odot})$	$\log(L_{\nu}/L_{\odot})$	$\log(T_{\text{eff}})$ (K)	$\log(T_c)$ (K)	$\log(\rho_c)$ (g/cm ³)	M_{cryst}/M	$\log(q_{\text{conv}})$	$\log(\text{Age})$ (years)
0.0	0.198	4.673	7.788	6.420	0.000	-14.765	$-\infty$
-0.1	0.098	4.651	7.777	6.424	"	-14.699	5.651
-0.2	-0.008	4.628	7.765	6.427	"	-14.627	5.988
-0.3	-0.119	4.605	7.753	6.430	"	-14.559	6.203
-0.4	-0.236	4.582	7.741	6.433	"	-14.512	6.368
-0.5	-0.360	4.559	7.727	6.436	"	-14.450	6.508
-0.6	-0.492	4.536	7.713	6.438	"	-14.390	6.635
-0.7	-0.635	4.513	7.696	6.441	"	-14.353	6.753
-0.8	-0.790	4.489	7.678	6.443	"	-14.298	6.868
-0.9	-0.963	4.466	7.658	6.445	"	-14.247	6.981
-1.0	-1.157	4.442	7.634	6.447	"	-14.193	7.096
-1.1	-1.375	4.419	7.607	6.449	"	-14.082	7.214
-1.2	-1.623	4.395	7.576	6.452	"	-13.825	7.335
-1.3	-1.902	4.371	7.541	6.454	"	-13.219	7.458
-1.4	-2.218	4.348	7.502	6.456	"	-12.448	7.581
-1.5	-2.562	4.324	7.459	6.457	"	-11.840	7.700
-1.6	-2.919	4.300	7.415	6.459	"	-11.166	7.811
-1.7	-3.319	4.276	7.371	6.461	"	-10.104	7.913
-1.8	-3.735	4.252	7.326	6.462	"	-9.037	8.007
-1.9	-4.159	4.228	7.281	6.463	"	-8.371	8.095
-2.0	-4.580	4.204	7.237	6.465	"	-7.766	8.175
-2.1	-4.960	4.180	7.196	6.466	"	-7.237	8.246
-2.2	-5.335	4.155	7.156	6.466	"	-6.840	8.315
-2.3	-5.700	4.131	7.115	6.467	"	-6.536	8.382
-2.4	-6.077	4.107	7.074	6.468	"	-6.300	8.449
-2.5	-6.759	4.082	7.034	6.468	"	-6.094	8.515
-2.6	< -7.0	4.058	6.994	6.469	"	-5.904	8.581
-2.7	"	4.033	6.953	6.470	"	-5.703	8.646
-2.8	"	4.009	6.911	6.470	"	-5.523	8.713
-2.9	"	3.984	6.868	6.471	"	-5.383	8.782
-3.0	"	3.960	6.821	6.471	"	-5.309	8.853
-3.1	"	3.935	6.774	6.471	"	-5.296	8.924
-3.2	"	3.910	6.724	6.472	"	-5.306	8.997
-3.3	"	3.886	6.675	6.472	"	-5.326	9.069
-3.4	"	3.861	6.619	6.473	0.141	-5.326	9.156
-3.5	"	3.837	6.544	6.473	0.426	-5.296	9.259
-3.6	"	3.812	6.463	6.473	0.586	-5.369	9.342
-3.7	"	3.787	6.403	6.474	0.646	-5.389	9.401
-3.8	"	3.762	6.341	6.474	0.760	-5.424	9.458
-3.9	"	3.737	6.280	6.474	0.842	-5.458	9.510

TABLE II
(continued)

$\log(L/L_{\odot})$	$\log(L_{\nu}/L_{\odot})$	$\log(T_{\text{eff}})$ (K)	$\log(T_c)$ (K)	$\log(\rho_c)$ (g/cm ³)	M_{cryst}/M	$\log(q_{\text{conv}})$	$\log(\text{Age})$ (years)
-4.0	< -7.0	3.713	6.218	6.474	0.901	-5.492	9.556
-4.1	"	3.688	6.160	6.474	0.922	-5.538	9.597
-4.2	"	3.663	6.105	6.474	0.934	-5.573	9.635
-4.3	"	3.638	6.047	6.474	0.942	-5.573	9.675
-4.4	"	3.613	5.983	6.475	0.947	-5.519	9.715
-4.5	"	3.588	5.082	6.475	0.950	-5.435	9.754
-4.6	"	3.563	5.918	6.475	0.952	-5.331	9.790
-4.7	"	3.538	5.790	6.475	0.954	-5.240	9.823
-4.8	"	3.513	5.731	6.475	0.956	-5.184	9.851
-4.9	"	3.488	5.647	6.475	0.959	-5.166	9.877
-5.0	"	3.463	5.620	6.475	0.968	-5.172	9.902
-5.1	"	3.438	5.564	6.475	0.982	-5.189	9.926
-5.2	"	3.413	5.507	6.475	0.990	-5.203	9.948
-5.3	"	3.388	5.450	6.475	0.995	-5.214	9.968
-5.4	"	3.363	5.392	6.475	0.997	-5.225	9.986
-5.5	"	3.338	5.333	6.475	0.999	-5.241	10.003
-5.6	"	3.313	5.276	6.475	0.999	-5.265	10.017
-5.7	"	3.288	5.227	6.475	0.999	-5.291	10.028
-5.8	"	3.263	5.162	6.475	0.999	-5.174	10.042

approximation in the interior of WDs where the bulk of their mass is located. In fact, this Figure shows the density profile of the interior of four Chandrasekhar's WD models (1939) plotted against the dimensionless radial coordinate η . For the values of the parameter $y_0 = 0.1, 0.4, 0.6,$ and 0.8 , they correspond to masses of (assuming the absence of hydrogen in the interior) $M = 1.08, 0.612, 0.405,$ and $0.22M_{\odot}$ respectively. This justifies the validity of our approximation.

The growth of the fraction of the crystallized phase with respect to the luminosity, considering an isothermal interior, is:

$$\frac{d}{d \log L} \left(\frac{M_{\text{cryst}}}{M} \right) = \frac{1}{M} 4\pi \rho_{\text{cryst}} r^2 \frac{dr}{d\rho} \Big|_{\text{front}} \frac{d\rho_{\text{cryst}}}{dT_*} \frac{dT_*}{d \log L}, \quad (6)$$

where ρ_{cryst} is the density at the crystallization front. In the approximation in which we are working, we obtain*

$$M = \pi^{3/2} a^3 \rho_0 \quad (7)$$

* In getting Equation (7) we have extended the upper limit of the integral to infinity. This introduces a completely negligible error.

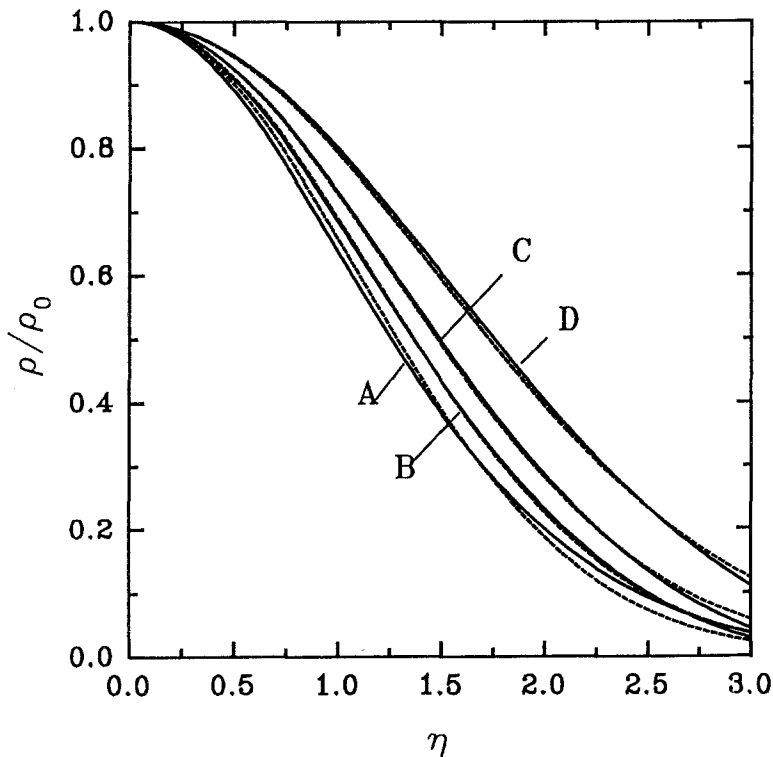


Fig. 4. The density profile of the white dwarf interior (solid lines) and the gaussian approximation given by Equation 5 (short dashed lines) vs. the transformed radial coordinate (see text). The letters A, B, C, and D correspond to $y_c = 0.1; 0.4; 0.6; 0.8$; and (assuming the absence of hydrogen in the interior) $M = 1.08; 0.612; 0.405; 0.22M_\odot$.

$$\frac{dr}{d\rho} = -\frac{a^2}{2r\rho} \quad (8)$$

$$\frac{d\rho_{\text{cryst}}}{dT_*} = \frac{3\rho_{\text{cryst}}}{T_*}. \quad (9)$$

Replacing in Equation (6), we have

$$\frac{d}{d \log L} \left(\frac{M_{\text{cryst}}}{M} \right) = -\frac{6 \ln 10}{\alpha \sqrt{\pi}} \left(\frac{\rho_{\text{cryst}}}{\rho_0} \right) \ln^{1/2} \left(\frac{\rho_0}{\rho_{\text{cryst}}} \right). \quad (10)$$

Using Equations (3) and (4), we can also write

$$\frac{\rho_{\text{cryst}}}{\rho_0} = \left(\frac{T_{\text{cryst}}}{T_0} \right)^3 = \left(\frac{L}{L_0} \right)^{3/\alpha} \quad (11)$$

where T_0 and L_0 are the internal temperature and luminosity respectively at the onset of crystallization.

If we define ψ so that

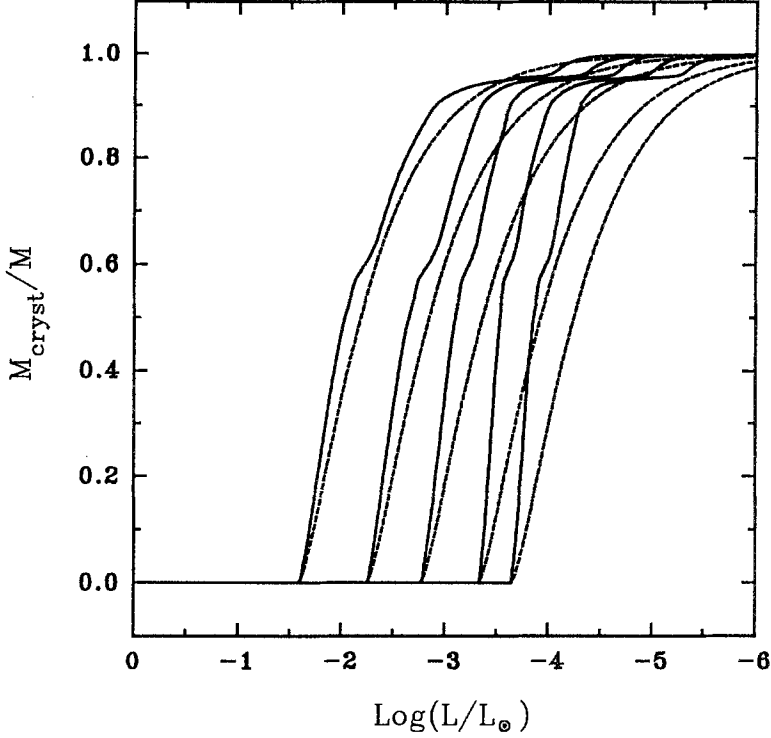


Fig. 5. The same as Figure 3 together with the analytical model in the case of the Mestel's value $\alpha = 7/2$. Solid and short dashed lines correspond to the numerical and the analytical model respectively.

$$L = L_0 \exp(-\psi), \quad (12)$$

we arrive at a differential equation

$$\frac{d}{d\psi} \left(\frac{M_{\text{cryst}}}{M} \right) = \frac{2}{\sqrt{\pi}} \left(\frac{3}{\alpha} \right)^{3/2} \sqrt{\psi} \exp(-3\psi/\alpha), \quad (13)$$

which is independent of L_0 and gives a family of curves to one parameter which is just L_0 . This equation can be easily integrated and we arrive at the theoretical crystal growth function

$$\frac{M_{\text{cryst}}}{M} = \text{erf} \left(\sqrt{\frac{3\psi}{\alpha}} \right) - 2\sqrt{\frac{3\psi}{\pi\alpha}} \exp \left(-\frac{3\psi}{\alpha} \right), \quad (14)$$

where, as usual, the error function is given by

$$\text{erf}(x) = \frac{2}{\sqrt{\pi}} \int_0^x \exp(-t^2) dt. \quad (15)$$

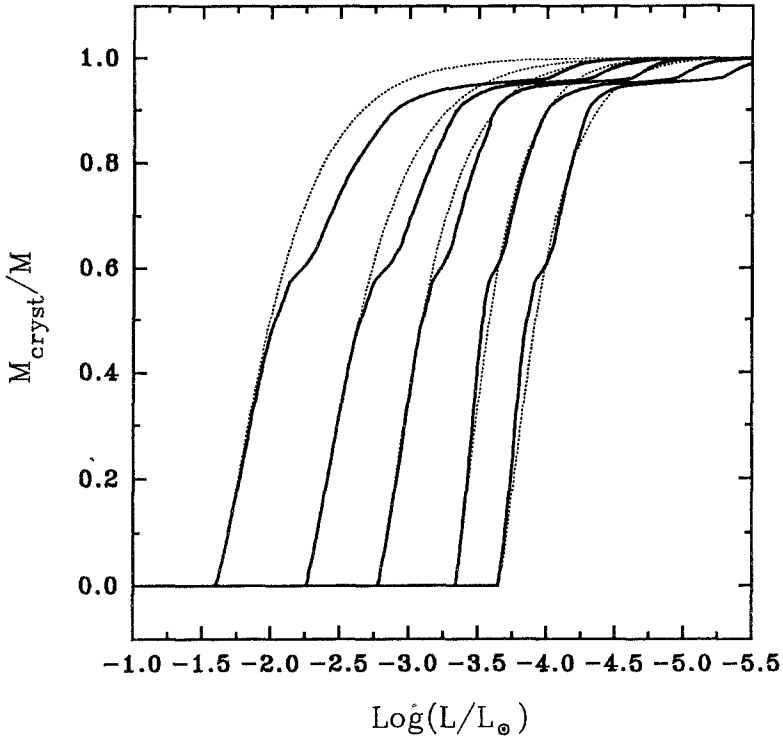


Fig. 6. The same as Figure 5 but employing the values of α given in Table I.

In Figure 5, we show the analytic function describing the growth of the crystallized phase for the case of Kramers opacities ($\alpha = 3.5$) together with the numerical results. We have set L_o as the same found in numerical calculations for each model. We note that the agreement is reasonable for massive models, but is poorer the lower the model mass.

Our numerical study strongly suggests that there exist a relationship $L \propto T_*^\alpha$ in more general conditions than previously assumed (e.g. opacities not given by Equation (2), convective layers, etc.). Allowing for such a relationship we can interpret the parameter α as an *effective* one for the non-degenerate envelope and then, we recover Equation (14) for the growth of the crystal phase. In Figure 6, we present the growth of crystal employing the values of α given in Table I together with the results of Section 3. These values have been calculated from the numerical study from the beginning of crystallization until $M_{\text{cryst}}/M = 0.8$ is reached. It is clearly noticeable that the agreement is better by far compared to the case of Figure 5, especially if we remember that in the analytic treatment we have assumed a homogeneous WD interior.

Finally, in Figure 7, we show the results for the crystallization of WDs whose interior ($M_r \leq 0.995M$) are composed only by ^{12}C and ^{16}O in equal fractions. As

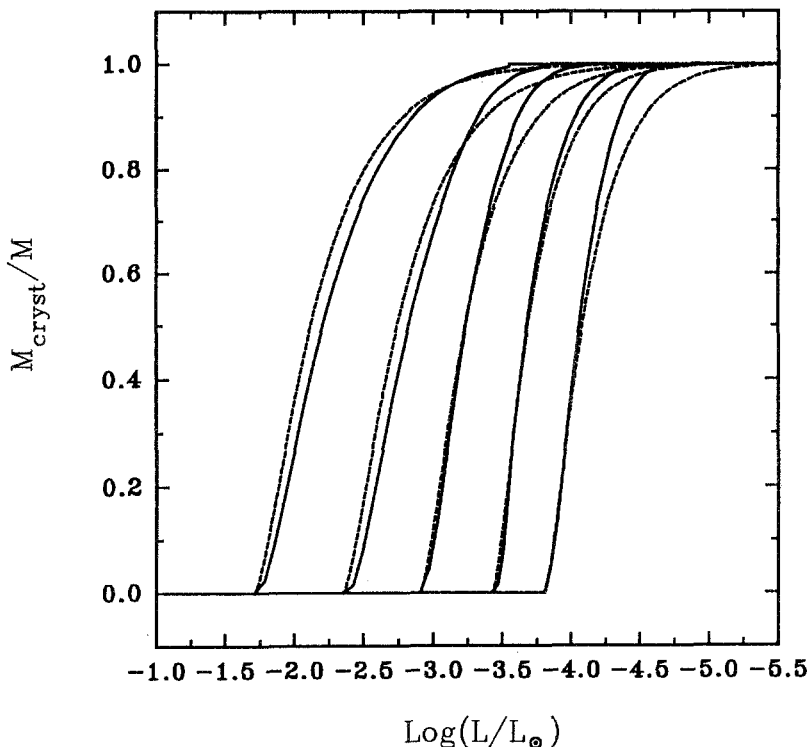


Fig. 7. The same as Figure 6 but employing numerical results of white dwarf interior composed by ^{12}C and ^{16}O in equal fractions.

expected, the agreement between the numerical and the analytical study is better than in the other non-homogeneous cases here presented.

5. Discussion and Conclusions

We have applied a full stellar evolution code in order to study the evolution of non-DA WD models with masses of 0.4 , 0.55 , 0.8 , 1.0 , and $1.2M_{\odot}$. We paid special attention to the behaviour of the crystallization front. The results presented here show that the shape of the crystal growth function is very similar for the WDs we studied, almost independent of the value of the total stellar mass.

We also studied the crystallization process analytically. The numerical results are nicely accounted for by a very simple model. If we assume Kramers opacities and neglect latent heat release and convection (Mestel Theory) the agreement between the numerical and the analytical results is reasonable for the most massive model, but gets poorer the lower the model mass is (Figure 5). This is just what we would expect because the effects of convection and latent heat release are indeed

negligible only for massive models. In fact, for example, all the crystallization epoch of $0.4M_{\odot}$ WD occurs in the convective envelope regime.

If we assume that α in $L \propto T_*^{\alpha}$ is variable, then by fitting to the numerical models we implicitly include all the phenomena neglected before. This relationship is much more accurate (especially for low mass WD) than $\alpha = 3.5$. Then, it is not surprising that the agreement between the results given by Equation (14) and the numerical study is much better than the one shown in Figure 5. In the case of numerical studies of homogeneous WD models, like those presented in Figure 7, the agreement between numerical and analytical calculations improves significantly, as expected.

Acknowledgements

We are deeply indebted to Profs. F. D'Antona and I. Mazzitelli for sending us the initial model and the Equation of State for the low density regime. O.G.B. is deeply indebted to Prof. A. Feinstein for making it possible for him to stand the great effort that was spent on writing this evolutionary code. We also thank to our Referee, Dr. M.A. Wood for his reports which allowed us to improve the quality of the first version of this work. This work has been partially supported by the Comisión de Investigaciones Científicas de la Provincia de Buenos Aires and the Consejo Nacional de Investigaciones Científicas y Técnicas (Argentina).

References

- Benvenuto, O.G.: 1988, *Ph.D. thesis*, Facultad de Ciencias Astronómicas y Geofísicas (UNLP).
- Bergeron, P., Saffer, R.A. and Liebert, J.: 1992, *Astrophys. J.* **394**, 228.
- Chabrier, G.: 1993, *Astrophys. J.* **414**, 695.
- Chandrasekhar, S.: 1939, *An introduction to the study of stellar structure*, Univ. of Chicago Press.
- Cox, A. and Tabor, J.: 1976, *Astrophys. J. Suppl.* **31**, 271.
- D'Antona, F. and Mazzitelli, I.: 1989, *Astrophys. J.* **347**, 934.
- D'Antona, F. and Mazzitelli, I.: 1990, *Annu. Rev. Astron. Astrophys.* **28**, 139.
- D'Antona, F. and Mazzitelli, I.: 1994, *Astrophys. J. Suppl.* **90**, 467.
- Hansen, J.P.: 1973, *Phys. Rev. A* **8**, 3096.
- Hubbard, W.B. and Lampe, M.: 1969, *Astrophys. J. Suppl.* **18**, 297.
- Iben, I.: 1975, *Astrophys. J.* **196**, 525.
- Iglesias, C.A., Rogers, F.J. and Wilson, B.G.: 1992, *Astrophys. J.* **397**, 717.
- Iglesias, C.A. and Rogers, F.J.: 1993, *Astrophys. J.* **412**, 752.
- Itoh, N. and Kohyama, Y.: 1983a, *Astrophys. J.* **275**, 858.
- Itoh, N., Mitake, S., Iyetomi, H. and Ichimaru, S.: 1983b, *Astrophys. J.* **273**, 774.
- Itoh, N., Kohyama, Y., Matsumoto, N. and Seki, M.: 1984, *Astrophys. J.* **285**, 758.
- Itoh, N., Adachi, T., Nakagawa, H., Kohyama, Y. and Munakata, H.: 1989, *Astrophys. J.* **339**, 354.
- Itoh, N., Mutoh, H. and Hikita, A.: 1992, *Astrophys. J.* **395**, 622.
- Itoh, N. and Kohyama, Y.: 1993, *Astrophys. J.* **404**, 268.
- Kippenhahn, R., Weigert, A. and Hofmeister, E.: 1967, *Methods in computational Physics* **7**, B. Alder, S. Fernbach and M. Rottenberg (eds.), Academic Press, New York.
- Koester, D. and Chanmugam, G.: 1990, *Rep. Prog. Phys.* **53**, 837.
- Kovetz, A., Lamb, D.Q. and Van Horn, H.M.: 1972, *Astrophys. J.* **174**, 109.

- Liebert, J., Dahn, C. and Monet, D.: 1988, *Astrophys. J.* **332**, 891.
- Lamb, D.Q. and Van Horn, H.M.: 1975, *Astrophys. J.* **200**, 306.
- Magni, G. and Mazzitelli, I.: 1979, *Astron. and Astrophys.* **72**, 134.
- Mestel, L.: 1952, *Monthly Notices Roy. Astron. Soc.* **112**, 583.
- Mestel, L. and Ruderman, M.A.: 1967, *Monthly Notices Roy. Astron. Soc.* **136**, 27.
- Munakata, H., Kohyama, Y. and Itoh, N.: 1987, *Astrophys. J.* **316**, 708.
- Ogata, S. and Ichimaru, S.: 1987, *Phys. Rev. A* **36**, 5451.
- Rogers, F.J. and Iglesias, C.A.: 1992, *Astrophys. J. Suppl.* **79**, 507.
- Schwarzschild, M.: 1958, *Structure and Evolution of the Stars*, Princeton Univ. Press.
- Shapiro, S.L. and Teukolsky, S.A.: 1983, *Black Holes, White Dwarfs and Neutron Stars. The Physics of Compact Objects*, Wiley-Interscience, New York.
- Shaviv, G. and Kovetz, A.: 1972, *Astron. and Astrophys.* **16**, 72.
- Van Horn, H.M.: 1968, *Astrophys. J.* **151**, 227.
- Wood, M.A.: 1992, *Astrophys. J.* **386**, 539.